

2014

Numerical Simulation Of Three-dimension Unsteady Flow In The Compression Chambers Of A Scroll Compressor

Shuanglai Liu

Compressor and Motor Institute of Gree Electric Appliances, Inc. of Zhuhai, China, People's Republic of,
shuanglai89@163.com

Xiaoli Kang

Compressor and Motor Institute of Gree Electric Appliances, Inc. of Zhuhai, China, People's Republic of

Caixia Shan

Compressor and Motor Institute of Gree Electric Appliances, Inc. of Zhuhai, China, People's Republic of

Yusheng Hu

Compressor and Motor Institute of Gree Electric Appliances, Inc. of Zhuhai, China, People's Republic of

Follow this and additional works at: <https://docs.lib.purdue.edu/icec>

Liu, Shuanglai; Kang, Xiaoli; Shan, Caixia; and Hu, Yusheng, "Numerical Simulation Of Three-dimension Unsteady Flow In The Compression Chambers Of A Scroll Compressor" (2014). *International Compressor Engineering Conference*. Paper 2277.
<https://docs.lib.purdue.edu/icec/2277>

This document has been made available through Purdue e-Pubs, a service of the Purdue University Libraries. Please contact epubs@purdue.edu for additional information.

Complete proceedings may be acquired in print and on CD-ROM directly from the Ray W. Herrick Laboratories at <https://engineering.purdue.edu/Herrick/Events/orderlit.html>

Numerical Simulation of Three-dimension Unsteady Flow in the Compression Chambers of a Scroll Compressor

Shuanglai Liu, Xiaoli Kang, Caixia Shan, Yusheng Hu

Compressor and Motor Institute of Gree Electric Appliances, Inc. of Zhuhai,
Jinji West Rd., Zhuhai City, 519070, P. R. China
Phone: +86-756-8974653, Fax: +86-756-8668386,
E-mail: shuanglai89@163.com

ABSTRACT

Due to the movement of orbiting scroll and leakage in scroll compressor chambers, the unsteady flow has significant influence on compression process. It's necessary to takes account of both flow and thermodynamics process in analysis of compression. This paper has carried out a numerical simulation of the whole compression process in scroll compressor, involving suction, compression and discharge process. By solving mass, momentum and energy equations of the refrigerant, the velocity, pressure and temperature distribution in all compression chambers throughout the entire compression cycle has been obtained, which takes account of all the influence of flow and thermodynamics process. The field quantities have shown nonuniform distribution in every compression chamber, and leakage between different chambers is obvious. Further, the overall parameters, such as mass flow rate and compression power consumption, have been calculated from the field quantities. The general comparisons between numerical and experimental results show a reasonable good agreement. The research is useful for the optimal design of the compressor geometric structure.

1. INTRODUCTION

Energy-saving and environment protection becomes the most serious problem in recent days. The scroll compressor, as a positive displacement machine with high efficiency and less noise, is very popular and widely used in air-conditioning and refrigeration industry. With the increasing need of developing more efficient and reliable scroll compressor, it requires more effort to study the details of scroll compressor.

In scroll compressor, several crescent-shaped chambers have been isolated by delicate designed orbiting scroll wrap and fixed scroll wrap. With the movement of orbiting scroll, the compression chamber from outside of the scroll is gradually squeezed towards discharge chamber and the refrigerant is compressed. During the compression process, the flow field in working chamber continues to move and deform, which shouldn't be neglected in most situation of analysis. But the compression process is so complex that it still poses a great challenge for numerical simulation of the unsteady, three-dimensional, compressible flow in a scroll compressor. To simplify the problem, the flow and heat transfer could be computed using one-dimensional flow models with various empirical correlations (Chen,2002 and Winandy,2002). However, these empirical correlations are usually not suitable well for different structure and operating condition, and one-dimensional flow models only focus on the averaged quantities in working chamber. The details of flow and heat transfer can not be presented, and also it is difficult to carry out the further analysis, such as force and thermal deformation.

In this paper, a numerical simulation has been developed to study the whole compression process in scroll compressor. The real movement and shape deformation of the working chamber has been realized with the moving mesh method provided by commercial CFD software. This research is expected to provide a description and analysis of field quantities within the scroll compressor, which could be useful for the further optimal design of the compressor geometric structure.

2. PHYSICAL MODEL OF SCROLL COMPRESSOR

Figure 1 shows the configuration of the scroll compressor. The refrigerant flows into the compressor through the suction port. And then, with the movement of orbiting scroll which is driven by the crank shaft, the refrigerant is compressed. After the compression process is over, the refrigerant is discharged into compressor shell through the discharge port of the fixed scroll. The compression process is demonstrated in Figure 2. From outer periphery to center, there are three pairs of chamber, the suction, first, second gas chamber and one discharge chamber. It takes two orbiting cycles from the gas pockets finishing suction to the refrigerant discharged. The starting step 0° is defined as the moment when the outermost chambers are sealed off. As refrigerant moves towards the center, the compression chambers continue deforming and moving, and the trapped gas is compressed. The discharge step begins at about 482° , while the compression chambers reach the center of the scrolls and the tip of orbiting scroll is unable to cover the discharge port of the fixed scroll. The discharge process will continue to next cycle. The main geometric and operating parameters of the scroll compressor studied in this paper are presented in Table 1.

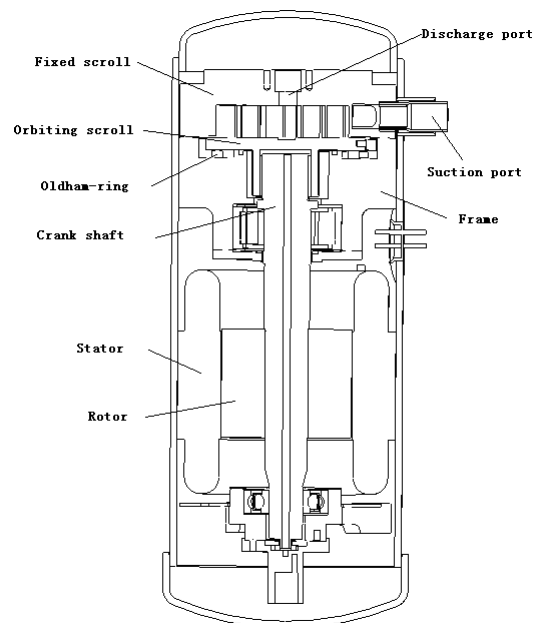


Figure 1: Geometry of scroll compressor

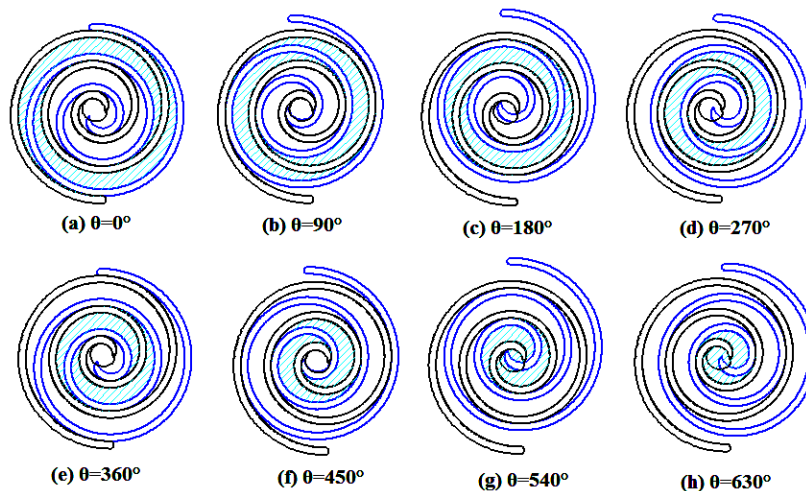


Figure 2: Compression process

Table 1: Main parameters of scroll compressor

parameter	Value
Displacement volume [cm ³]	55
Wrap thickness [mm]	4
Wrap Height[mm]	27.3
Nominal speed [rpm]	3600.0
Refrigerant	R410a
Evaporating temperature [°C]	7.2
Condensing Temperature [°C]	54.4
Suction Temperature [°C]	18.3

3. NUMERICAL SIMULATION PROCEDURE

When the refrigerant flows into the working chamber, it shows strong transient phenomena with the scroll orbiting. The pressure, density and temperature of the refrigerant significant change as the volume of working chamber decreases. The governing equations are time dependant and involving mass, momentum and energy conservation equations. The mass and momentum equations for transient compressible fluid flows, as known as the Navier-Stokes equations, can be expressed in Cartesian tensor notation (Warsi, 1981):

$$\frac{\partial \rho}{\partial t} + \frac{\partial}{\partial x_j} (\rho u_j) = 0 \quad (1)$$

$$\frac{\partial \rho u_i}{\partial t} + \frac{\partial}{\partial x_j} (\rho u_j u_i - \tau_{ij}) = -\frac{\partial p}{\partial x_i} + s_i \quad (2)$$

Heat transfer is solved through the following general form of the enthalpy conservation equation (Jones, 1980):

$$\frac{\partial \rho h}{\partial t} + \frac{\partial}{\partial x_j} \left(\rho h u_j - \frac{k_{eff}}{c_p} \frac{\partial h}{\partial x_j} \right) = \frac{\partial p}{\partial t} + u_j \frac{\partial p}{\partial x_j} + \tau_{ij} \frac{\partial u_i}{\partial x_j} + s_h \quad (3)$$

The standard k-ε model is used to solve the turbulent flow. Transport equations for turbulence kinetic energy and dissipation rate are as follows (El Tahry, 1983)

$$\frac{\partial \rho k}{\partial t} + \frac{\partial}{\partial x_j} \left[\rho k u_j - \left(\mu + \frac{\mu_t}{\sigma_k} \right) \frac{\partial k}{\partial x_j} \right] = \mu_t \left(s_{ij} \frac{\partial u_i}{\partial x_j} - \frac{g_i}{\sigma_{h,t}} \frac{1}{\rho} \frac{\partial p}{\partial x_i} \right) - \rho \varepsilon - \frac{2}{3} \left(\mu_t \frac{\partial u_i}{\partial x_i} + \rho k \right) \frac{\partial u_i}{\partial x_i} + \mu_t P_{NL} \quad (4)$$

$$\frac{\partial \rho \varepsilon}{\partial t} + \frac{\partial}{\partial x_j} \left[\rho \varepsilon u_j - \left(\mu + \frac{\mu_t}{\sigma_\varepsilon} \right) \frac{\partial \varepsilon}{\partial x_j} \right] = C_{\varepsilon 1} \frac{\varepsilon}{k} \left[\mu_t P - \frac{2}{3} \left(\mu_t \frac{\partial u_i}{\partial x_i} + \rho k \right) \frac{\partial u_i}{\partial x_i} \right] + C_{\varepsilon 3} \frac{\varepsilon}{k} \mu_t P_B - C_{\varepsilon 2} \rho \frac{\varepsilon^2}{k} + C_{\varepsilon 4} \rho \varepsilon \frac{\partial u_i}{\partial x_i} + C_{\varepsilon 1} \frac{\varepsilon}{k} \mu_t P_{NL} \quad (5)$$

The computational domain includes the suction port, working chambers and discharge port. A Structured mesh is generated for the flow field, and the total mesh has about 300,000 hexahedral elements. A moving mesh method is used to regenerate the mesh for the domain involving scrolls at every time step. In computational model, the axial clearance of scroll is neglected, but the radial clearance is reserved. And the flow field is only occupied by refrigerant, without lubricating oil considered.

The pressure boundary condition is applied on inlet and outlet, which is equal to 0.997MPa (evaporating temperature 7.2 °C) and 3.36MPa (condensing temperature 54.4 °C) respectively. The inlet has constant suction temperature of 18.3 °C. The scroll wrap is considered as smooth no-slip and adiabatic wall. The varying velocity boundary is imposed on orbiting scroll wrap, according to the rotational speed of the crank shaft.

Governing equations are dispersed using finite volume method (FVM) and algebraic equations are solved by PISO algorithm. The solution is considered as convergence when normalized absolute residual sum over all cells in the computational domain is reduced to 10^{-3} and 10^{-2} for pressure and other variables at every time step, respectively. The thermodynamic and transport properties of R410A are calculated by REFPROP 9.0 which is developed by National Institute of Standards and Technology (NIST, USA).

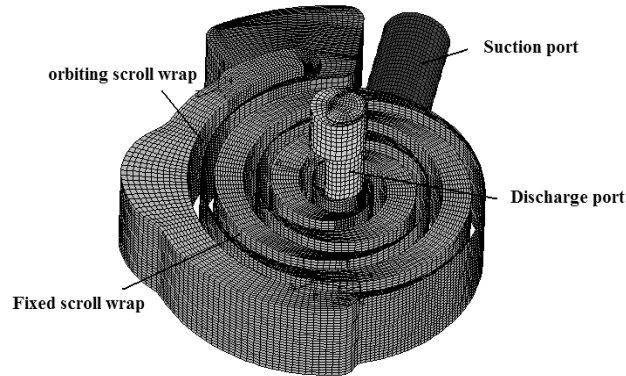


Figure 3: Mesh for computational domain

4. RESULTS VALIDATION AND DISCUSSIONS

4.1 Results validation

An experiment test has been carried out under the operating condition shown in Table 1. The numerical and experiment results about mass flow rate and isentropic efficiency have been compared to validate the numerical simulation. The isentropic efficiency η_i can be defined as follow

$$\eta_i = \frac{w_{is}}{w_{cp}} = \frac{h_{in} - h_{dis,is}}{h_{in} - h_{dis,act}} \quad (6)$$

Where W_{is} is isentropic compression power, W_{cp} is actual compression power, h_{in} is specific enthalpy of inlet, $h_{dis,is}$ is isentropic specific enthalpy of discharge gas, $h_{dis,act}$ is actual specific enthalpy of discharge gas. In numerical simulation, the compression power W_{cp} is directly obtained from the work that is done by gas pressure on the orbiting scroll.

Figure 4 shows the compared results while the scroll compressor running at different rotational speed. The numerical results of mass flow rate are slightly higher than experiment, and the most deviation is lower than 3.2%. The differences between numerical and experiment results about isentropic efficiency are less than 3.5%, as shown in Figure 4(b).

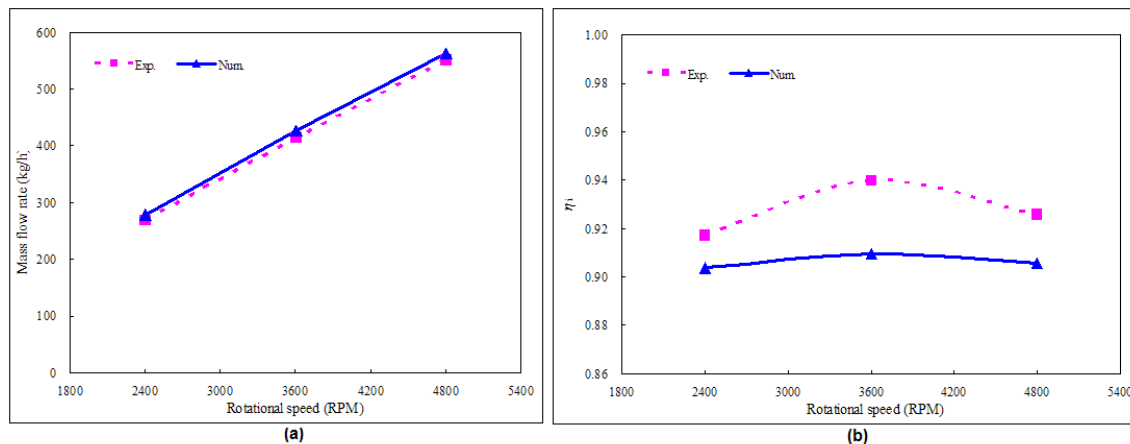


Figure 4: Comparison of experiment and simulation: (a) mass flow rate, (b) isentropic efficiency

4.2 Flow characteristic in working chambers

Figure 5 shows the overall characteristics of the flow field. Although each pair of working chamber presents a general symmetric flow, the slightly difference still could be found in some parts of the flow field. The leakage is significant in compression chamber and the pressure difference causes gas flow into downstream chamber while other gas flow from upstream chamber. From outer to the center of scroll wrap, the pressure and temperature increase gradually.

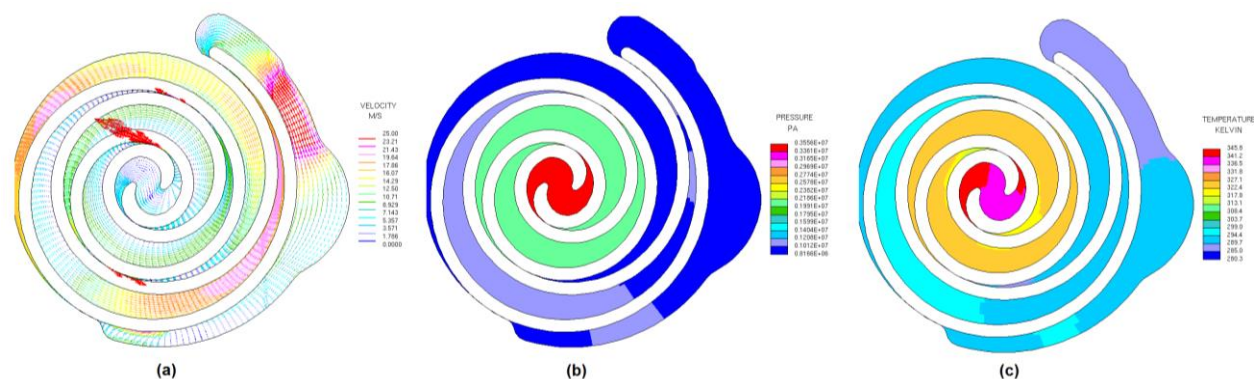


Figure 5: Overall characteristic of the flow field: (a) velocity, (b) pressure, (c) temperature

The velocity, pressure and temperature distribution in one working chamber from initial step $\theta=0^\circ$ to step $\theta=360^\circ$ are shown in Figure 6-8. With the movement of the working chamber, the refrigerant flows from outer corner to inner corner of the crescent chamber and the velocity finally decreases meanwhile. Also, the leakage flow is found in both corners of the chamber, and it seems more significant as the chamber is approaching the center of involute.

The movement of scroll wrap and the leakage between chambers have important influence on the flow field. The pressure and temperature along chamber both show nonuniform distribution. It should be noted that the pressure of the chamber at initial step $\theta=0^\circ$ is actually higher than suction pressure, which means the refrigerant is already slightly compressed before the compression step starts due to the orbiting of scroll. And this feature of pre-compression results a slightly higher volumetric efficiency than theoretical analysis could be found in scroll compressor if the leakage is small enough to be neglected. As shown in Figure 8, the leakage has significant influence on temperature distribution, and it conduces to more nonuniform phenomenon than pressure distribution, especially at the tip of chamber.

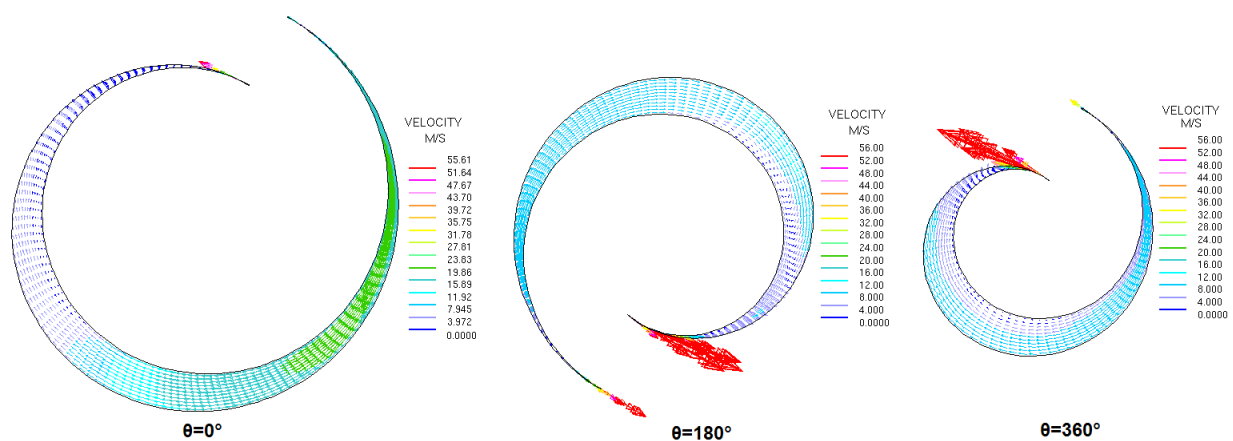


Figure 6: Velocity of the working chamber

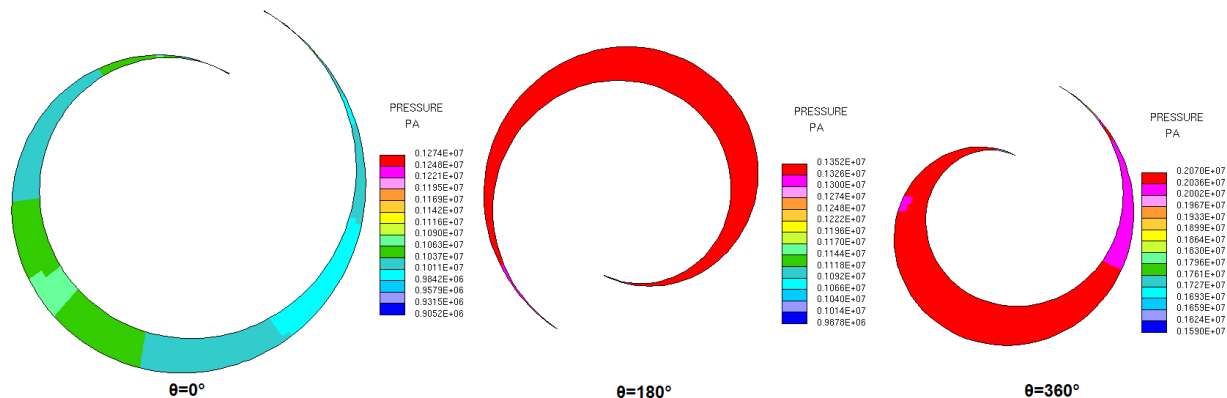


Figure 7: Pressure of the working chamber

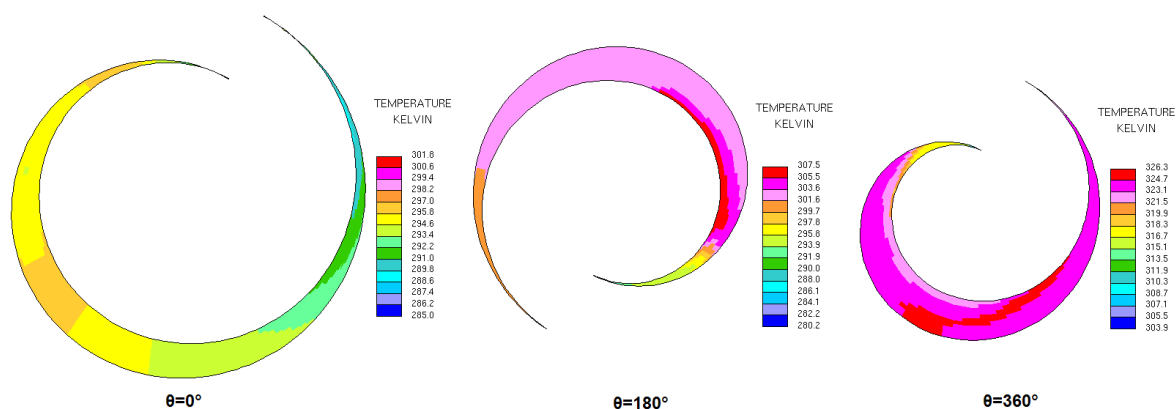


Figure 8: Temperature of the working chamber

4.3 Gas forces on orbiting scroll

Several forces and moment are acting on orbiting scroll during the compression. As seen in Figure 9, the gas forces mainly consist of axial, radial and tangential force. The horizontal forces, including radial and tangential force, cause the overturning moment. These forces have a very important influence on the friction loss and the reliability of the scroll compressor. The overturning moment raises a trend of tipping the orbiting scroll and increases the clearance between scrolls, which could result in more friction and leakage loss in scroll compressor.

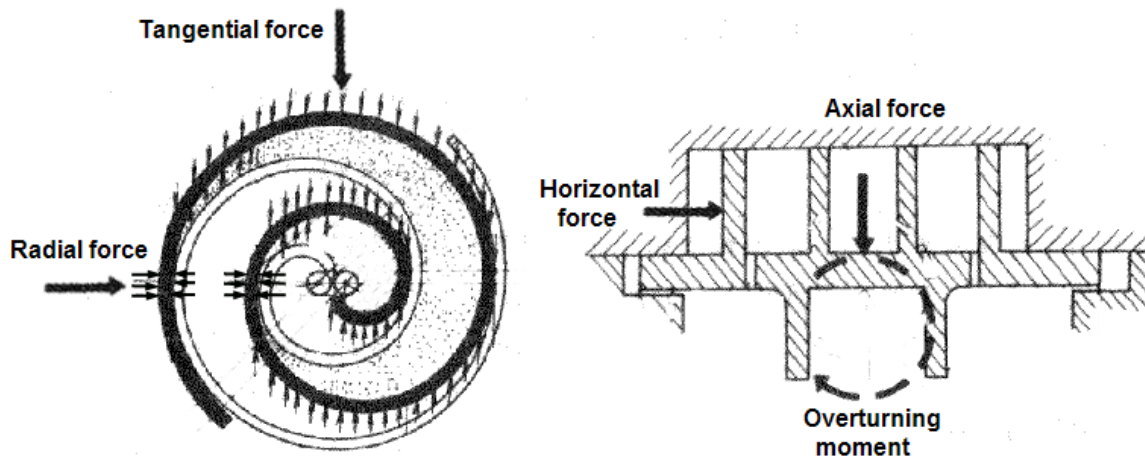


Figure 9: Illustration of gas forces on orbiting scroll

Figure 10 shows the forces and overturning moment curves acting on orbiting scroll in two orbiting cycles. Obviously, all curves periodically change with the rotation of crank shaft. The axial and tangential force first increase as the compression process continues, and they reach the peak at about $\theta=210^\circ$ in every orbiting cycle. The under-compression process actually occurs in compressor at current operating conditions. It means the pressure of second compression chamber is lower than discharge pressure when compression step is ending, and after that the second compression chamber is merged into discharge chamber. Thus, the compression still continues until discharge chamber achieves terminal pressure at the beginning of discharge step. Once discharge chamber reaches the final pressure, as discharge process continues, the axial and tangential force begins to decrease. Also, as is seen, the tangential and radial force fluctuates rapidly, whereas the axial force is more like a smooth curve. In traditional analysis, uniform pressure distribution is assumed in compression chamber. The tangential and radial force need only consider the gas pressure acting on some parts of scroll as shown in Figure 9, while the pressure of rest parts can be eliminated with each other. However, pressure distribution has significant difference in the compression chamber, as discussed above. As the orbiting scroll moves, the variety of pressure distribution causes the fluctuation of tangential and radial force. The overturning moment basically depends on tangential force, which has the similar feature with tangential force as seen in Figure 10(b).

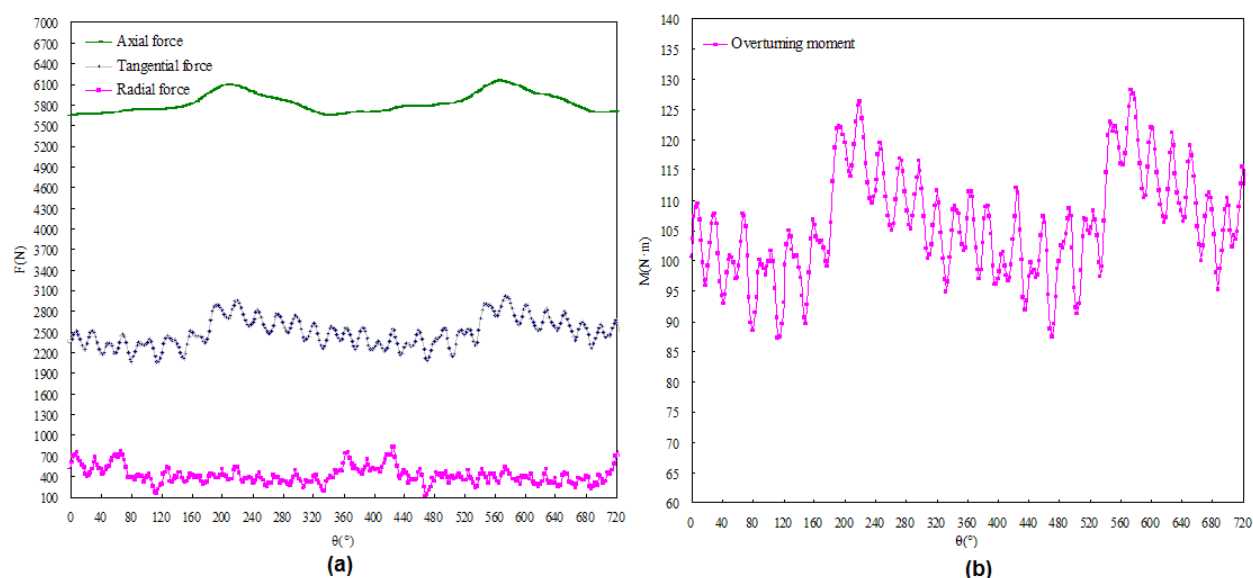


Figure 10: Gas forces and moment: (a) axial, radial and tangential force, (b) overturning moment

5. CONCLUSION

A numerical simulation has been developed to study the unsteady three-dimensional compressible flow in scroll compressor. By solving mass, momentum and energy equations of the refrigerant, the velocity, pressure and temperature distribution in all compression chambers throughout the entire compression cycle has been obtained.

The numerical and experiment results about mass flow rate and isentropic efficiency show a reasonable good agreement. The numerical results of mass flow rate are slightly higher than experiment, and the most deviation is lower than 3.2%. The differences between numerical and experiment results about isentropic efficiency are less than 3.5%.

The field quantities have shown nonuniform distribution in compression chamber, which is mainly caused by the movement and leakage. The leakage flow is significant in compression chamber, especially as the chamber is approaching the center of involute. Due to the orbiting of scroll, the refrigerant is already slightly compressed before the compression step starts. The axial, radial and tangential forces on orbiting scroll periodically change with the rotation of crank shaft, and the nonuniform distribution of pressure causes the fluctuation of tangential and radial force.

REFERENCES

- Chen, Y., Halm, N. P., Groll, E. A., and Braun, J. E., 2002. Mathematical Modeling of Scroll Compressors. Part I: Compression Process Modeling. *International Journal of Refrigeration*, vol. 25:p.731–750.
- Winandy, E. L., and Lebrun J., 2002. Scroll compressors using gas and liquid injection: experimental analysis and modeling. *International Journal of Refrigeration*, vol. 25:p.1143–1156.
- Warsi, Z.V.A., 1981. Conservation form of the Navier-Stokes equations in general nonsteady coordinates. *AIAA, Journal*, vol.19:p.240-242.
- Jones, W. P., 1980. *Prediction methods for turbulent flames*. Hemisphere, Washington, D.C., 1-45.
- El Tahry, S. H., 1983. k- ϵ equation for compressible reciprocating engine flows. *AIAA, J. Energy*, vol.7, no.4:p. 345–353.